Marijan Herceg, Mario Vranješ, Drago Žagar

Performance of Multi Pulse Position Amplitude Modulation for TH IR-UWB Communication Systems

Original scientific paper

The multi pulse position amplitude modulation scheme for time-hopping multiple access impulse radio ultra-wideband communication systems has been presented in this paper. Multi pulse position amplitude modulation is a hybrid modulation technique, which combines multi pulse position modulation and pulse amplitude modulation. It is shown that multi pulse position amplitude modulation significantly outperforms pulse position modulation with respect to bandwidth efficiency. The multi pulse position amplitude modulation error probability over IEEE 802.15.3a multipath fading channels in multiuser environment is derived. The system analysis shows that the proper selection of modulation parameters can improve the system performance at the cost of hardware complexity (and vice versa).

Key words: Ultra-wideband, Multi pulse position modulation, Pulse amplitude modulation, Multipath channel

Performanse višeimpulsno-pozicijske amplitudne modulacije za TH IR-UWB komunikacijske sustave. U ovom je radu predstavljena višeimpulsno-pozicijska amplitudna modulacijska shema za impulsne ul-traširokopojasne radiokomunikacijske sustave, zasnovana na višekorisničkom pristupu s vremenskim skaka-njem. Višeimpulsno-pozicijska amplitudna modulacija je hibridni modulacijski postupak, koji je kombinacija višeimpulsno-pozicijske modulacije i impulsno-amplitudne modulacije. Pokazano je da višeimpulsno-pozicijska amplitudna modulacija značajno nadmašuje impulsno-pozicijsku modulaciju u pogledu pojasne učinkovitosti. Izve-dena je vjerojatnost pogreške višeimpulsno-pozicijske amplitudne modulacije u kanalu IEEE 802.15.3a s višes-taznim rasprostiranjem i iščezavanjem signala u višekorisničkom okruženju. Analiza sustava pokazuje da odgo-varajući izbor parametara modulacije može poboljšati performanse sustava uz povećanje složenosti sklopovlja (i obrnuto).

Ključne riječi: ultra-široki pojas, višeimpulsno-pozicijska modulacija, impulsno-amplitudna modulacija, kanal s višestaznim rasprostiranjem

1 INTRODUCTION

Impulse radio ultra-wideband (IR-UWB) [1] systems have recently gained increased popularity due to their low power consumption, high speed transmission and anti-interference characteristics. In IR-UWB systems, symbols are transmitted with very short pulses (< 2 ns), which implies a large signal bandwidth. Different modulation techniques such as pulse amplitude modulation (PAM), pulse position modulation (PPM), pulse interval modulation (PIM) [2], pulse shape modulation (PSM), on-off-keying (OOK) and bi-phase shift keying (BPSK) are used to transmit the information in such systems. To achieve a better system performance such as a higher data rate, a less complex receiver and less power consumption, combined modulation techniques such as pulse position amplitude modulation (PPAM) [3], biorthogonal pulse posi-tion modulation (BPPM) [4], OOK-PSM [5], PPM-PSM [6] and hybrid amplitude shape modulation (h-ASM) [7], are proposed. In PAM and OOK modulation, the information is conveyed in the amplitude of the signal, PPM uses the position of the pulse to convey the information, while in PSM the information is conveyed in the shape of the pulse.

In PPM, the information which is carried within the symbol is determined by the position of one pulse. Furthermore, N-ary PPM requires N correlators in the optimal receiver, which significantly increases the hardware complexity. To solve these problems and to increase the transmission data rate, the multi pulse position amplitude modulation (MPPAM) scheme [8], which is based on the simultaneous position and amplitude level of the multiple pulses, is proposed.

This paper is organized as follows. Section 2 describes

the basic properties of the MPPAM modulation scheme. In Section 3 the multipath fading channel is described and error probability and performance bounds of a MPPAM UWB systems in multi user environment are derived. Section 4 shows numerical results of the MPPAM system performance and the conclusions are given in Section 5.

2 MPPAM BASICS

Multi pulse position modulation (MPPM) [9] was first derived for optical wireless communication systems to increase the bandwidth efficiency. In MPPM each symbol consists of w pulses positioned in N different time slots, which gives the overall symbol set size of

$$C_w^N = \frac{N!}{w!(N-w)!}. \tag{1}$$

C_w^N is rarely a power of two, so b data bits are encoded in the MPPM symbol subset of size

$$2^{\left\lfloor \log_2 C_w^N \right\rfloor}, \tag{2}$$

where $\lfloor \cdot \rfloor$ is the integer floor operator. Introducing the M-ary PAM, MPPM becomes MPPAM and the symbol set size is M^w times increased, so then the overall number of bits mapped with one symbol is

$$b = \left\lfloor \log_2 \left(M^w \times C_w^N \right) \right\rfloor, \tag{3}$$

The modulation bandwidth efficiency is defined as $\eta_{B-MPPAM} = R_{b-MPPAM}/B$, where $R_{b-MPPAM}$ is a MPPAM bit-rate written as

$$R_{b-MPPAM} = \frac{\left\lfloor \log_2 \left(M^w \times C_w^N \right) \right\rfloor}{NT_p}, \tag{4}$$

$B \approx 1/T_p$ is the channel bandwidth, while T_p is the pulse duration.

In Fig. 1 the bandwidth efficiency of MPPAM and BPPM normalized to PPM bandwidth efficiency is shown. It can be seen that MPPAM significantly outperforms PPM and BPPM regarding to bandwidth efficiency, especially for the higher number of bits per symbol.

3 MPPAM PERFORMANCE AND CHANNEL MODEL

In the case where one pulse per symbol is transmitted, the so called *catastrophic collision*, where pulses from several transmitters arrive at the receiver at the same time, can occur because the fact that UWB transceivers are unsynchronized. This leads to a lower system performance. To avoid that, time-hopping (TH) format for IR-UWB is proposed. In such format each data symbol is represented by
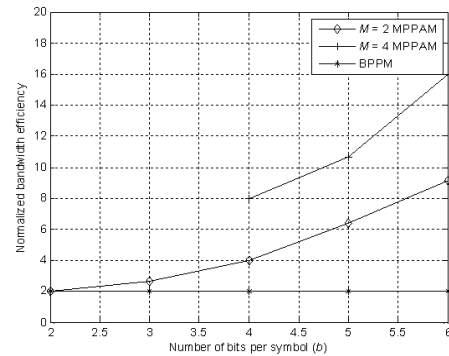
Fig. 1. Normalized bandwidth efficiency of BPPM and MP-PAM with w=2, M=2 and M=4

several pulses. According to a TH code, the transmitted pulse sequence is different for each user. Therefore, even if one pulse within a symbol collides with a signal component from another user, other pulses in the sequence will not. Finally, the possibility of catastrophic collision is significantly reduced.

If TH format is considered, the TH IR-MPPAM signal for the k-th user can be written as

$$s^{(k)}(t) = \sum_{j=-\infty}^{\infty} \sum_{i=0}^{w-1} A_{z_{i,\left\lfloor \frac{j}{N_s} \right\rfloor}^{(k)}} \sqrt{\frac{E_t}{N_s w}}$$
$$\cdot p(t - jT_f - c_j^{(k)}T_c - d_{i,\left\lfloor \frac{j}{N_s} \right\rfloor}^{(k)} \frac{T_c}{N}), \tag{5}$$

where $z_{i,\lfloor j/N_s \rfloor}^{(k)} \in \{1, 2, ..., M\}$, $d_{i,\lfloor j/N_s \rfloor}^{(k)} \in \{0, 1, ..., N-1\}$, $A_{z_{i,\lfloor j/N_s \rfloor}} \sqrt{E_t/(N_s w)}$ is one of the possible amplitude levels with $A_{z_{i,\lfloor j/N_s \rfloor}^{(k)}} = 2z_{i,\lfloor j/N_s \rfloor}^{(k)} - 1 - M$. $E_t = 3E_{av}/(M^2 - 1)$ is the pulse energy, where E_{av} is the average energy of the pulse and T_f is the frame time. Each frame is divided into N_h chips with duration of T_c. $c_j^{(k)}$ is the TH code for k-th user which takes integer value in the range of $0 \le c_j^{(k)} \le N_h - 1$. It provides the additional shift in order to avoid the catastrophic collisions due to multi-user interference (MUI), where N_h is chosen to satisfy the condition $N_h T_c \le T_f$. Each chip (T_c) is divided into N slots with duration of $T_p = T_c/N$. N_s is the frame repetition interval, and the overall symbol period is then $T_s = N_s T_f$. $p(t)$ is a Gaussian monocycle which is defined in [10] as

$$p(t) = \left[1 - 4\pi \left(\frac{t}{\tau_p} \right)^2 \right] \exp \left[-2\pi \left(\frac{t}{\tau_p} \right)^2 \right], \tag{6}$$

where τ_p is the time normalization factor. Defining the au-

tocorrelation function of $p(t)$ as

$$R(x) = \int_{-\infty}^{\infty} p(t)p(t-x)dt, \tag{7}$$

it can be written as

$$R(x) = \left[1 - 4\pi\left(\frac{x}{\tau_p}\right)^2 + \frac{4\pi^2}{3}\left(\frac{x}{\tau_p}\right)^4\right] \\ \cdot \exp\left[-\pi\left(\frac{x}{\tau_p}\right)^2\right]. \tag{8}$$

In the IEEE 802.15.3a channel model presented in [11], the multipath components arrive in clusters and channel impulse response can be written as

$$h(t) = \sum_{l=0}^{L}\sum_{k=0}^{K} \alpha_{k,l}\delta(t - T_l - \tau_{k,l}), \tag{9}$$

where $\alpha_{k,l}$ is the gain coefficient of k-th ray in l-th cluster, $\tau_{k,l}$ is the arrival time of k-th ray relative to cluster's arrival time T_l, while $\delta(\cdot)$ is a Dirac's delta function. The arrival times of clusters and rays are modeled as Poisson distributions, where the cluster and ray arrival rates are denoted by Λ and λ, respectively. Moreover, the multipath gain coefficient $\alpha_{k,l}$ can be divided in two components as $\alpha_{k,l} = p_{k,l}\beta_{k,l}$, where $p_{k,l}$ accounts for signal inversion due to the reflection with equiprobably values of ± 1 and $\beta_{k,l}$ is a log-normal random variable, denoted by $20\log(\beta_{k,l}) \propto N(\mu_{k,l}, \sigma^2)$. The power delay profile decays double exponentially, and the second moment of the amplitude attenuation can be expressed as $E(\beta_{k,l}^2) = \Omega_0 \exp(-T_l/\Gamma)\exp(-\tau_{k,l}/\gamma)$, where Ω_0 is the mean power of the first ray of the first cluster, Γ and γ are power decay factors of the cluster and ray, respectively.

The analysis of the interference statistics based on this channel model is complicated due to the random arrival times of clusters and rays. Thus, an equivalent discrete channel model as the one described with (9) was proposed in [12], where the arrival time axis is divided into time bins with duration of Δ. When this channel model is used, in any time bin one or more multipath components can arrive due to the cluster overlapping. Then the channel gain coefficients of all arrived multipath components are added together to yield a combined channel coefficient. This discrete channel model for the k-th user can be represented as

$$h^{(k)}(t) = \sum_{l=1}^{L_t} \alpha_l^{(k)}\delta(t - l\Delta), \tag{10}$$

where L_t is the total number of available multipath components, $\alpha_l^{(k)}$ represents the sum of multipath coefficients

arrived in l-th time bin, Δ is the time bin duration chosen to be less than the delay spread, so that the $\left\{\alpha_l^{(k)}\right\}_{l=1}^{L_t}$ related to the different time bins can be considered as uncorrelated. In order to avoid the pulse distortion due to the partial pulse overlapping, the pulse-width T_p should be very small (less then 0.167 ns). With such small pulse-width, the (10) will be good approximation of (9).

If we assume that the first user is the desired user and that the signal delay of the first user is zero, the received signal, based on the discrete time channel model described with (10), can be written as

$$r(t) = \sum_{l=1}^{L_t} \alpha_l^{(1)}s^{(1)}(t - l\Delta) \\ + \sum_{k=2}^{N_u}\sum_{l=1}^{L_t} \alpha_l^{(k)}s^{(k)}(t - l\Delta - \tau_k) + n(t), \tag{11}$$

where N_u is the number of users, $n(t)$ is additive white Gaussian noise (AWGN) modeled as Gaussian random process with power spectral density of $N_0/2$.

Due to the robustness of UWB signals to multipath, high diversity order can be exploited with the adoption of the RAKE receiver. RAKE receiver, which employs the maximal-ratio combining (MRC), will collect reflected and delayed versions of the transmitted signal and it will combine them in order to achieve the better performance. Assuming that the channel parameters are perfectly known at the receiver and that TH sequence of first user is $c_j^{(1)} = 0$ for all j, the template signal of i-th branch for first user can be written as

$$v_i(t) = \sum_{l=1}^{L_p} \alpha_l^{(1)}\sum_{m=0}^{N_s-1} p_i(t - mT_f - l\Delta), \tag{12}$$

where L_p is the number of RAKE fingers, and $p_i(t)$ is

$$p_i(t) = p(t - (i-1)\frac{T_c}{N}). \tag{13}$$

MRC RAKE based correlator receiver is shown in Fig. 2.

In order to derive the analytical symbol error rate (SER) expression for MPPAM, the TH IR-UWB system in which all symbols are equiprobable is assumed and it is also assumed that the 0-th transmitted information symbol is sent. Furthermore it is assumed that the sent symbol contains pulses with the m-th amplitude level in the first w slots followed by $(N-w)$ empty slots (which means that $d_{0,0}^{(1)} = 0, d_{1,0}^{(1)} = 1, ..., d_{w-1,0}^{(1)} = w - 1, z_{0,0}^{(1)} = ... = z_{w-1,0}^{(1)} = m$). In this case, the outputs of the bank of N MRC RAKE based correlators shown in Fig. 2 can be char-
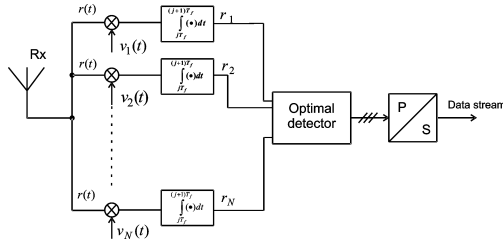
Fig. 2. MRC RAKE based correlator receiver

acterized by the vector $\boldsymbol{r} = [r_1 \ r_2 \ ... \ r_N]$, where r_i is

$$r_i = \int_0^{T_s} r(t)v_i(t)dt = \begin{cases} S_i + I_i + n_i, & 1 \le i \le w \\ I_i + n_i, & w+1 \le i \le N \end{cases} \tag{14}$$

In (14) S_i is the channel averaged contribution of desired signal component at i-th correlator and it is given by

$$S_i = A_{z_{i,0}^{(1)}} \sqrt{\frac{E_t N_s}{w}} \sum_{l=1}^{L_p} E((\alpha_l^{(1)})^2), \tag{15}$$

where $E(*)$ is the mean value operator and $E((\alpha_l^{(1)})^2)$ is defined in [12]. n_i is the filtered AWGN term at the i-th correlator with zero mean and variance

$$\sigma_{n_i}^2 = \frac{N_0}{2} N_s \sum_{l=1}^{L_p} E((\alpha_l^{(1)})^2). \tag{16}$$

I_i is the MUI at the i-th correlator which can be expressed as

$$I_i = \sum_{l=1}^{L_p} \alpha_l^{(1)} \sum_{k=2}^{N_u} \sum_{m=0}^{N_s-1} \sum_{l_1=1}^{L_t} \sum_{j=-\infty}^{\infty} \sum_{i'=0}^{w-1} A_{z_{i',\lfloor j/N_s \rfloor}^{(k)}}$$
$$\cdot \sqrt{\frac{E_t}{N_s w}} \alpha_{l_1}^{(k)} R_i((j-m)T_f + c_j^{(k)}T_c + (l_1-l)\Delta$$
$$+ \tau_k + d_{i',\lfloor \frac{j}{N_s} \rfloor}^{(k)} \frac{T_c}{N}), \tag{17}$$

where $R_i(x)$ is the autocorrelation at i-th correlator. As it is mentioned earlier, the amplitudes $\left\{ \alpha_l^{(k)} \right\}_{l=1}^{L_t}$ have zero mean, so the probability density function (PDF) of MUI is symmetric around zero. In order to derive the second moment of MUI, the assumption

$$N_h T_c \le \frac{T_f}{2} - 2T_p - T_m \tag{18}$$

is adopted [10, 12], where T_m is the channel delay spread. Denoting the time shift from (17) $(l_1-l)\Delta + \tau_k$ as $\tau_{l_1,l,k}$, it can be modeled as [13]

$$\tau_{l_1,l,k} = (l_1-l)\Delta + \tau_k = j_{l_1,l,k}T_f + \beta_{l_1,l,k}, \tag{19}$$

where $j_{l_1,l,k}$ is the time shift of k-th user rounded to the nearest frame time, while $\beta_{l_1,l,k}$ is the error in rounding process which is modeled as random variable uniformly distributed over interval $[-T_f/2, T_f/2]$. Then the autocorrelation function $R_i(x)$ from (17) can be written as

$$R_i((j + j_{l_1,l,k} - m)T_f + c_j^{(k)}T_c + \beta_{l_1,l,k} + d_{i',\lfloor \frac{j}{N_s} \rfloor}^{(k)} \frac{T_c}{N}). \tag{20}$$

Due to the (18) and the property that autocorrelation function is nonzero only for $|x| < T_p$, there is only one nonzero term in summation over frame index j in (17) and it satisfies the condition $j + j_{l_1,l,k} - m = 0$. The second moment conditioned on $c_j^{(k)}, \beta_{l_1,l,k}, d_{i',\lfloor j/N_s \rfloor}^{(k)}, z_{i',\lfloor j/N_s \rfloor}^{(k)}$ can be written as

$$\sigma_{I_i}^2 = E(I_i^2 | c_j^{(k)}, \beta_{l_1,l,k}, d_{i',\lfloor j/N_s \rfloor}^{(k)}, z_{i',\lfloor j/N_s \rfloor}^{(k)})$$
$$= \sum_{l=1}^{L_p} E((\alpha_l^{(1)})^2) \sum_{k=2}^{N_u} \sum_{m=0}^{N_s-1} \sum_{l_1=1}^{L_t} \sum_{i'=0}^{w-1} E(A_{z_{i',\lfloor j/N_s \rfloor}^{(k)}}^2 \frac{E_t}{N_s w})$$
$$\cdot E((\alpha_{l_1}^{(k)})^2) R_i^2(c_j^{(k)}T_c + \beta_{l_1,l,k} + d_{i',\lfloor \frac{j}{N_s} \rfloor}^{(k)} \frac{T_c}{N}). \tag{21}$$

Assuming that all amplitude levels are equiprobable, their second moment can be written as

$$E(A_{z_{i',\lfloor j/N_s \rfloor}^{(k)}}^2 \frac{E_t}{N_s w}) = \frac{E_{av}}{N_s w}. \tag{22}$$

The total channel energy is normalized to 1, what can be written as

$$\sum_{i=1}^{L_t} E((\alpha_{l_1}^{(k)})^2) = 1. \tag{23}$$

Furthermore, assuming that the TH sequence of k-th user can take the value of $\{0, 1, ..., N_h - 1\}$ with equal probability of $1/N_h$, $d_{i',\lfloor j/N_s \rfloor}^{(k)}$ can take the value of $\{0, 1,..., N\text{-}1\}$ with equal probability of $1/N$, and that $\beta_{l_1,l,k}$ is uniformly distributed over interval $[-T_f/2, T_f/2]$, by averaging these random variables in (21) the second moment of MUI, according to [13], can be then expressed as

$$\sigma_{I_i}^2 = E(I_i^2) = (N_u - 1)E_{av} \frac{1}{T_f} \int_{-\infty}^{\infty} R_i^2(t)dt$$
$$\cdot \sum_{l=1}^{L_p} E((\alpha_l^{(1)})^2). \tag{24}$$

Detector selects w correlators with the largest magnitude. After selection of the correlators with the largest magnitude, the sign and the value of that magnitude is used to decide which of the M possible amplitudes, i.e. m is sent.

In order to derive the error probability, firstly the probability that first pulse is detected correctly will be derived. From [3,14] this probability can be written as

$$P(c_1) = \frac{1}{M}$$

$$\times \left\{ \begin{array}{l} \sum_{m=2}^{M-1} \int_{(A_m-1)\sqrt{E_t/(N_s w)}}^{(A_m+1)\sqrt{E_t/(N_s w)}} \left(\prod_{z=w+1}^{N} \frac{1}{\sqrt{2\pi}} \right. \\ \left. \int_{-|bound|}^{|bound|} \exp(-\frac{x^2}{2})dx \right) \cdot p(r_1^{(m)})dr_1^{(m)} \\ + \int_{-\infty}^{(A_m+1)\sqrt{E_t/(N_s w)}} \left(\prod_{z=w+1}^{N} \frac{1}{\sqrt{2\pi}} \right. \\ \left. \int_{-|bound|}^{|bound|} \exp(-\frac{x^2}{2})dx \right) \cdot p(r_1^{(m)})dr_1^{(m)} \big|_{m=1} \\ + \int_{(A_m-1)\sqrt{E_t/(N_s w)}}^{\infty} \left(\prod_{z=w+1}^{N} \frac{1}{\sqrt{2\pi}} \right. \\ \left. \int_{-|bound|}^{|bound|} \exp(-\frac{x^2}{2})dx \right) \cdot p(r_1^{(m)})dr_1^{(m)} \big|_{m=M} \end{array} \right\},$$

(25)

where $r_1^{(m)}$ is the signal at the output of the first correlator when m-th amplitude level is sent, and

$$bound = \frac{\left|r_1^{(m)}\right|}{\sqrt{\sigma_{I_z}^2 + \sigma_{n_z}^2}},$$
$$p(r_1^{(m)}) = \frac{1}{\sqrt{2\pi\left(\sigma_{I_1}^2 + \sigma_{n_1}^2\right)}}$$
$$\cdot \exp\left(-\frac{\left(r_1^{(m)} - A_m\sqrt{\frac{E_t N_s}{w}}\sum_{l=1}^{L_p} E(\alpha_l^{(1)})^2\right)^2}{2(\sigma_{I_1}^2 + \sigma_{n_1}^2)} \right).$$

(26)

The expression for error probability can be extended to w pulses as

$$P(e) = 1 - \prod_{i=1}^{w} P(c_i).$$

(27)

4   NUMERICAL RESULTS

In this section, the numerical results from previously obtained expressions are presented and illustrated. The parameters for IEEE 802.15.3a channel models are given in [11]. As suggested in [11], the discrete time bin Δ is chosen to be 0.167 ns.

Figure 3 shows the analytical symbol error rate (SER) over channel model one (CM1) compared with Monte-Carlo simulation [15] for 2x2x4 (where this numbers mean $M \times w \times N$) and 2x2x8 MPPAM. It can be seen that the derived analytical expression for SER matches the Monte-Carlo simulation well for all signal-to-noise (SNR) ratios, which are defined as E_{avb}/N_0 ($E_{avb} = bE_{av}$). Figure 3 also indicates that the SER performance improves when frame repetition interval increases, as expected.

Figure 4 and Figure 5 show the influence of the number of RAKE fingers L_p on the SER for 2x2x4 MPPAM over CM1 and CM3, respectively. As expected, the SER
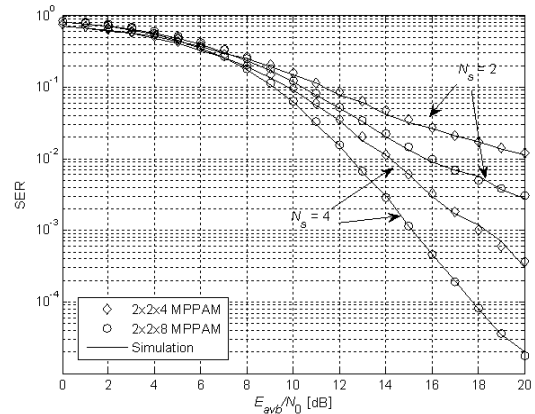
Fig. 3. SER of the TH MPPAM vs. SNR over CM1 for frame repetition interval $N_S = 2$, $N_S = 4$. Other system parameters are: $L_p = 10$, $N_h = 8$, $T_p = 0.167$ ns, $N_u = 10$, $T_f = 21$ ns for 2x2x4 MPPAM, and $T_f = 32$ ns for 2x2x8 MPPAM

performance increases when the L_p increases at the cost of higher hardware complexity. Note that SER performance of 2x2x4 MPPAM over CM1 is much better then over CM3, which is result of longer channel delay spread, as can be seen in [11].

Figure 6 shows the influence of different modulation parameters on SER performance for the fixed bit-rate set to 20 Mbps. It can be seen that 2x2x8 MPPAM has the better SER performance than 2x2x4 and 2x3x6 MPPAM. For example when SNR=12 dB, the SER of 2x2x8 MPPAM is $1*10^{-4}$, while the SER for 2x2x4 and 2x3x6 MPPAM is $1.2*10^{-3}$ and $7.5*10^{-4}$, respectively.

The comparison of MPPAM, PPM and PAM for the fixed bit-rate which is set to 20 Mbps is shown in Fig. 7. From that figure it can be seen that MPPAM achieves approximately 0.5 dB worse performance than PPM, while it significantly outperforms PAM. Generally, according to the expectation, it can be seen that the increasing of the MPPAM and PPM modulation level also improves the SER performance, while for PAM the SER performance deteriorates.

Figure 8 presents the user capacity vs. different values of SER for 2x2x4, 2x2x8, and 2x3x6 MPPAM. SNR is chosen to be 15 dB, and the bit-rate is set to 20 Mbps.

It can be seen that 2x2x8 MPPAM has the best SER for fixed number of users N_u. For example, if system supports 30 users, SER for 2x2x8 MPPAM is $7*10^{-5}$, for 2x2x4 and 2x3x6 MPPAM is $8*10^{-4}$ and $5.7*10^{-4}$, respectively. It is also shown that the SER increases as the number of users increases, as expected.
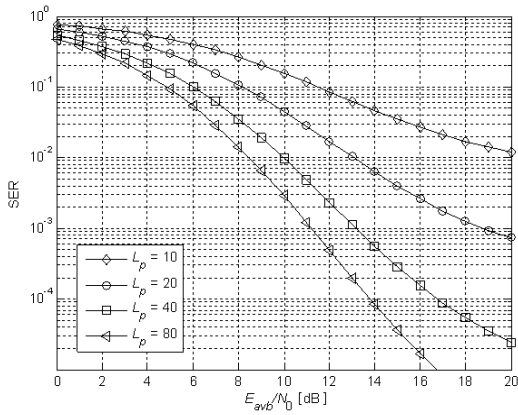
Fig. 4. SER of the 2x2x4 TH MPPAM over CM1 vs. SNR for different number of RAKE fingers Lp. Other system parameters are: N_h=8, T_p=0.167 ns, N_s=2, N_u=10, T_f=21 ns
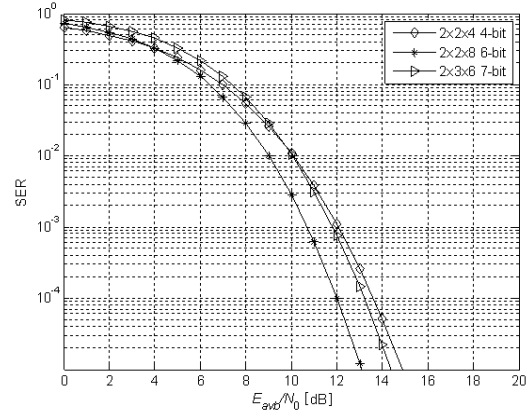
Fig. 6. SER of the 2x2x4 TH MPPAM over CM1 vs. SNR for different modulation parameters N and w. Other system parameters are: L_p=20, N_h=8, T_p=0.167 ns, N_s=2, N_u=10, bit-rate is 20 Mbps
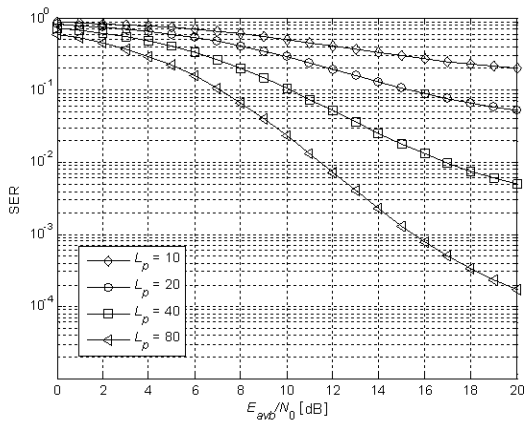
Fig. 5. SER of the 2x2x4 TH MPPAM over CM3 vs. SNR for different number of RAKE fingers L_p. Other system parameters are: N_h=8, T_p=0.167 ns, N_s=2, N_u=10, T_f=21 ns
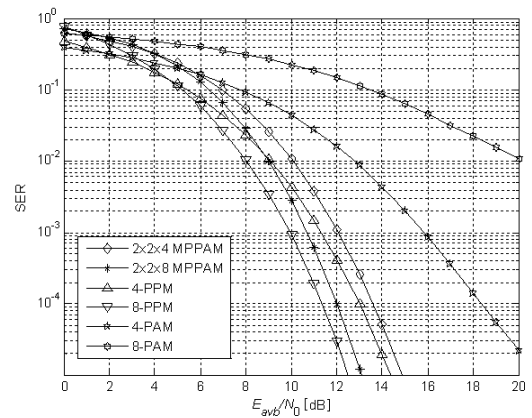
Fig. 7. SER of the MPPAM, PPM and PAM over CM1 vs. SNR. Other system parameters are: L_p=20, N_h=8, T_p=0.167 ns, N_s=2, N_u=10, bit- rate is 20 Mbps
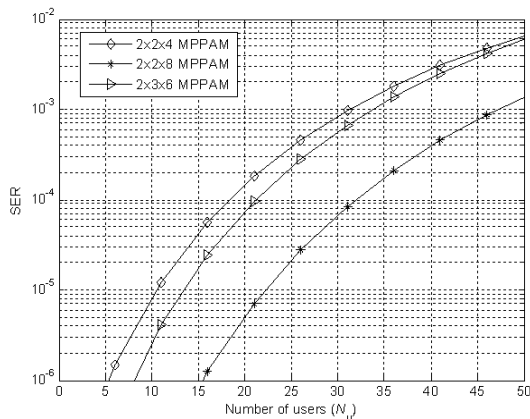
Fig. 8. SER of the MPPAM over CM1 vs. number of users N_u. Other system parameters are: L_p=20, N_h=8, T_p=0.167 ns, N_s=2, SNR=15 dB, bit-rate is 20 Mbps

5   CONCLUSION

This paper analyses the performance of the proposed MPPAM scheme over IEEE 802.15.3a channel models in multi-user environment. It can be seen that MPPAM significantly outperforms PPM and BPPM with respect to bandwidth efficiency when the number of bits per symbol increases. It is also shown that the receiver hardware complexity can be reduced if the number of pulses w increases, while the number of time slots N decreases (less number of receiver correlators), at the cost of the lower SER.

SER performance of MPPAM is compared to those of PAM and PPM for a fixed bit-rate. MPPAM provides significantly better performance than PAM and slightly worse than PPM, regarding the SER. Hence the advantage of MPPAM over PPM is that for a fixed symbol length N, MPPAM maps more bits per symbol than ordinary PPM, it has less hardware complexity and can achieve a higher bit-rates. These properties make the MPPAM scheme very attractive for TH IR-UWB short range communication systems.

REFERENCES

[1] R. A. Scholtz, "Multiple access with time-hopping impulse modulation", in *Proceedings of the IEEE Military Communications Conference*, (Cityplace-Boston, country-regionUSA), pp. 447-450, October 1993.

[2] M. Herceg, T. Švedek, and T. Matić, "Pulse Interval Modulation for Ultra-High Speed IR-UWB Communications Systems", *EURASIP Journal on Advances in Signal Processing*, vol. 2010, Article ID 658451, 8 pages, 2010. doi: 10.1155/2010/658451

[3] H. Zhang and T. A. Gulliver, "Pulse Position Amplitude Modulation for Time-Hopping Multiple-Access UWB Communicatios", *IEEE Transactions On Communications*, vol. 53, no. 8, pp. 1269-1273, 2005.

[4] H. Zhang and T. A. Gulliver, "Biorthogonal Pulse Position Modulation for Time-Hopping Multiple-Access UWB Communicatios", *IEEE Transactions On Wireless Communications*, vol. 4, no. 3, pp. 1154-1162, 2005.

[5] S. Majhi, A. S. Madhukumar, A.B. Premkumar and P. Richardson, "Combining OOK with PSM Modulation for TH-UWB Radio Systems: A Performance Analysis", *EURASIP Journal on Wireless Communications And Networking 2008*, pp. 1-11, 2008.

[6] C. J. Mitchell, G. Abreu and R. Kohno, "Combined Pulse Shape and Pulse Position Modulation for High Data Rate Transmissions in Ultra-Wideband Communications", *International Journal of Wireless Information Networks*, vol. 10, no. 4, pp. 167-178, 2003.

[7] M. Herceg, T. Matić and T. Švedek, "Performances of hybrid Amplitude Shape Modulation for UWB communications systems over AWGN channel in the single and multi-user environment", *Radioengineering Journal*, vol. 18, no. 3, pp. 265-271, 2009.

[8] M. Herceg, D. Žagar and D. Galić, "Multi Pulse Position Amplitude Modulation for ultra-high speed Time-Hopping UWB communication systems over AWGN channel", *4rd International Symposium on Communications, Control and Signal Processing*, (Limassol, Cyprus), pp. 1-4, March 2010.

[9] H. Sugiyama and K. Nosu, "MPPM: a method for improving the band-utilization efficiency in optical PPM", *Journal of Lightwave Techology*, vol. 7, pp. 465–472 , 1989.

[10] M. Z. Win and R. A. Scholtz, "Ultra-wide bandwidth time-hopping spread-spectrum impulse radio for wireless multiple-access communications", *IEEE Transactions On Communications*, vol. 48, no. 4, pp. 679–689, 2000.

[11] "Channel modeling sub-committee report final", IEEE P802.15-02/368r5-SG3a, December 2002.

[12] T. Jia and D. placeI. Kim, "Analysis of Channel-Averaged SINR for Indoor UWB Rake and Transmitted Reference Systems", *IEEE Transactions On Communications*, vol..55, no. 10, pp. 2022-2032, 2007.

[13] H. Shao and N. C. Beaulieu, "An analytical method for calculating the bit error rate performance of rake reception in UWB multipath fading channels", *IEEE Transactions On Communications*, vol. 58, no. 4, pp. 1112-1120, 2010.

[14] J. G. Proakis, *Digital Communications*, 4th edition, placeStateNew York: McGraw-Hill, 2001.

[15] J.G. Proakis and M. Salehi, *Contemporary Communication Systems Using MATLAB*, PWS publishing company, 1998.

Marijan Herceg was born in Osijek, Croatia in 1978. He received the B.S. and Ph.D degrees in electrical engineering from Faculty of Electrical Engineering in Osijek, Croatia in 2002 and 2010, respectively. He is currently assistant professor in the Department of Communications, Faculty of Electrical Engineering in Osijek, Croatia. His research interests are advanced modulation techniques for impulse radio ultrawideband (IR-UWB) systems, A/D conversion, sigma-delta A/D converters and FPGA programming for communications applications.

Mario Vranješ received the B.S. and Ph.D. degrees in electrical engineering from University of Osijek, Faculty of Electrical Engineering, in 2006 and 2012, respectively. He is currently assistant in the Dept. of Communications at the Faculty of Electrical Engineering in Osijek. His current research interests are video compression, video quality evaluation, multimedia broadcasting and wireless communication systems. He is a member of IEEE society.

Drago Žagar received the B.Sc., M.Sc. and Ph.D. from the University of Zagreb, Faculty of Electrical Engineering and Computing, in 1990, 1995, 2002, respectively. From the 1990 he was affiliated with the Department of Communications, Faculty of Electrical Engineering, University of Osijek, where he has reached a rank of associate professor. From 2003 to 2005 he was the Vice-Dean for education, and currently he is the Vice-Rector for education and students at the University of Osijek. His main research interests include Quality of Service in IP networks, formal methods for protocol verification, and computer networks. He has served in technical program committees of several conferences. He is a member of IEEE (Communication Society) and ACM.

AUTHORS' ADDRESSES
Asst. Prof. Marijan Herceg, Ph.D.
Asst. Mario Vranješ, Ph.D.
Full Prof. Drago Žagar, Ph.D.
Department of Communications,
Faculty of Electrical Engineering,
University of J.J. Strossmayer,
Kneza Trpimira 2b, 31000, Osijek, Croatia,
email: mherceg@etfos.hr, mario.vranjes@etfos.hr,
drago.zagar@etfos.hr